



We are Nitinol.™

**Oxidation of a NiTi Alloy**

Chan, Trigwell, Duerig

Surface and Interface Analysis

Vol. 5

pp. 349-354

1990

# Oxidation of an NiTi Alloy

C.-M. Chan, S. Trigwell and T. Duerig

Raychem Corporation, 300 Constitution Dr, Menlo Park, CA 94025, USA

In this study, the oxidation of the surface of a 50/50 (at.%) NiTi alloy was studied by XPS, AES and SEM. Samples of the NiTi alloy were oxidized at 23 °C and high temperatures at an oxygen pressure of  $10^{-4}$  Torr and in atmosphere. At  $10^{-4}$  Torr of  $O_2$  and 23 °C, titanium was oxidized preferentially while nickel remained in the metallic form even after 40 min of exposure. At the same oxygen partial pressure and 400 °C, a mixture of  $TiO_x$ ,  $Ti_2O_3$  and  $TiO_2$  was formed, and nickel remained metallic. Eventually, after 40 min of  $O_2$  exposure, the whole surface was covered with a layer of  $TiO_2$ . In atmosphere and at 23 °C, titanium again was oxidized preferentially, but NiO was detected on the surface after the first minute of air exposure. At a higher temperature of 450 °C, areas comprising a mixture of NiO and  $TiO_2$ , and areas consisting of  $TiO_2$  only were found. Below the top surface layer, a complete layer of  $TiO_2$  was detected. Underneath the  $TiO_2$  layer, a nickel-rich layer was present.

## INTRODUCTION

The oxidation and corrosion resistance of Ni alloys, such as NiCo,<sup>1-3</sup> NiCr,<sup>4,5</sup> NiCrFe,<sup>4</sup> NiAl<sup>6,7</sup> and Ni<sub>3</sub>Al,<sup>8</sup> are closely related to surface chemical reactions in different environments and at different temperatures. In a study of an NiCo alloy,<sup>3</sup> preferential oxidation and oxygen-induced segregation of Co were observed at 500 °C and  $10^{-5}$  Torr of oxygen. Oxidation of nickel was detected only after 4500 L (1 L =  $10^{-6}$  Torr-sec) of oxygen exposure. Preferential oxidation followed by oxygen-induced segregation of Cr was shown by Steffen and Hofmann<sup>4</sup> in an NiCr alloy at room temperature and low oxygen pressures ( $10^{-6}$ - $10^{-8}$  Torr). Nickel remained metallic until after 6-7 L of oxygen exposure. Preferential oxidation of Co and Cr over nickel is related to the relative magnitude of their free energies of formation. The effect of oxygen partial pressure on the oxidation of Ni<sub>3</sub>Al at temperatures above 600 °C has been studied by x-ray photoelectron spectroscopy (XPS) and Auger electron spectroscopy (AES).<sup>8</sup> At low oxygen pressure, only aluminum oxide was found. At atmospheric pressure, NiO, NiAl<sub>2</sub>O<sub>4</sub> and Al<sub>2</sub>O<sub>3</sub> were present.

The study of Ti and Ti alloys has gained importance because of numerous applications of Ti and its alloys in aerospace, chemical and medical industries.<sup>9</sup> The excellent corrosion-resistant properties and biocompatibility of Ti is closely related to the presence of a stable, passivating surface oxide film. Oxidation of Pt<sub>3</sub>Ti<sup>10</sup> at 377 °C and  $10^{-8}$  Torr of  $O_2$  produced a surface oxide layer composed mainly of  $TiO_2$ . Oxidation at a higher temperature (727 °C) and at a higher oxygen pressure ( $10^{-7}$  Torr) produced a new feature, which was identified as  $Ti^{3+}$  indicating the presence of defects or uncoordinated ions. In another study, the oxide layer produced by thermal and anodic oxidation of Ti-6Al-4V has been shown to be composed mainly of  $TiO_2$ .<sup>11</sup>

In this study, we examined the oxidation of NiTi by XPS, SEM and AES. The effect of temperature and oxygen pressure on the oxidation kinetics was also investigated.

## EXPERIMENTAL

To perform these experiments, a 1 cm<sup>2</sup> coupon (0.1 cm thick) of a 50/50 (at.%) NiTi alloy was abraded with a 600-grit SiC paper and polished with 0.3 μm alumina paste. Then the sample was ultrasonically cleaned in methanol. XPS experiments were performed in a VG Escalab Mk II spectrometer. The Au 4f<sub>7/2</sub> peak was set at 83.8 eV. The background pressure of the analysis and preparation chambers was  $10^{-9}$  and  $10^{-8}$  Torr, respectively. The sample was placed in a stainless-steel sample holder. Heating was done by putting the sample holder in a heating probe that is capable of heating up to 800 °C. Sample cleaning and sputtering were performed by a Commonwealth Scientific 3 cm ion source mounted in the preparation chamber or by an AG 61 ion gun mounted in the analysis chamber. The 3 cm ion source was operated at 500 V and  $2 \times 10^{-4}$  Torr of Ar with a beam current of 12.5 mA, while the AG 61 ion gun was operated at 5 kV and  $10^{-5}$  Torr of Ar with a sample current of 3 μA. The sputtering rate of the 3 cm ion source was calibrated to be 144 Å min<sup>-1</sup> for an Au standard. At the start of each experiment, the surface was sputter-cleaned with the 3 cm ion source until the surface chemical composition became constant.

## CONCLUSIONS

### Surface composition after sputter-cleaning

Figure 1 shows XPS spectra of the NiTi surface after the sample was sputter-cleaned in the preparation chamber with the 3 cm ion source at room temperature for 15 min (all spectra shown are in arbitrary units). The surface chemical composition was calculated using the peak areas corrected with empirically derived sensitivity factors.<sup>12</sup> The surface Ni concentration (55 at.%) is slightly higher than that of the bulk, indicating preferential sputtering of Ti (surface concentration of Ti was

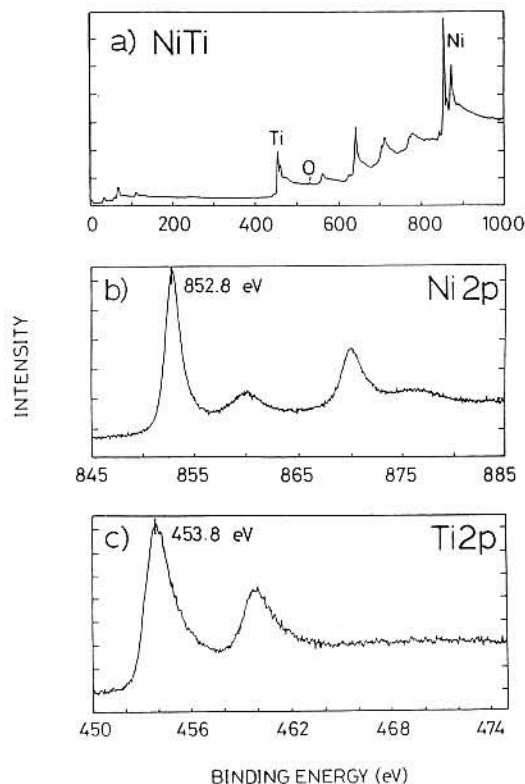


**Figure 1.** (a) An XPS spectrum of a sputter-cleaned NiTi surface; (b) Ni 2p spectrum for the same surface; (c) Ti 2p spectrum for the same surface.

41 at.%). In addition, a small amount of oxygen (4 at.%) was found. The binding energy of Ni and Ti was measured to be 852.8 and 453.8 eV, respectively. These results agree well with published values for these metals,<sup>13</sup> and there is no binding energy shift detected for either Ni or Ti. This is contrary to a previous soft x-ray appearance-potential study of NiTi alloys, which has reported that the binding energy of both Ni and Ti is shifted to a higher value as compared to those obtained in pure metals.<sup>14</sup>

#### Low oxygen pressure ( $10^{-4}$ Torr $O_2$ ) oxidation

**Room temperature.** After the surface of the alloy was sputter-cleaned with the 3 cm ion source for 15 min, the surface still had a small amount of oxygen associated with  $TiO_x$ . The sample was then exposed to  $10^{-4}$  Torr of  $O_2$  for various lengths of time. The oxygen concentration increased fairly rapidly during the first minute and stayed approximately constant afterwards, while the Ti/Ni concentration ratio was not changed significantly even after 40 min of oxygen exposure. However, a close examination of the Ti 2p spectra, as shown in Fig. 2, indicates that oxidation of Ti has occurred with the appearance of two new peaks—one at 454.3 eV indicating the formation of  $TiO_x$  and the another at 458.2 eV indicating the presence of  $TiO_2$ . The binding energies of different titanium oxides available in the literature are summarized in Table 1. Most of the  $TiO_x$  and  $TiO_2$  was developed during the first 10 min of oxygen exposure, and the amount grew very slowly afterwards. Oxidation of Ni was not detected even at

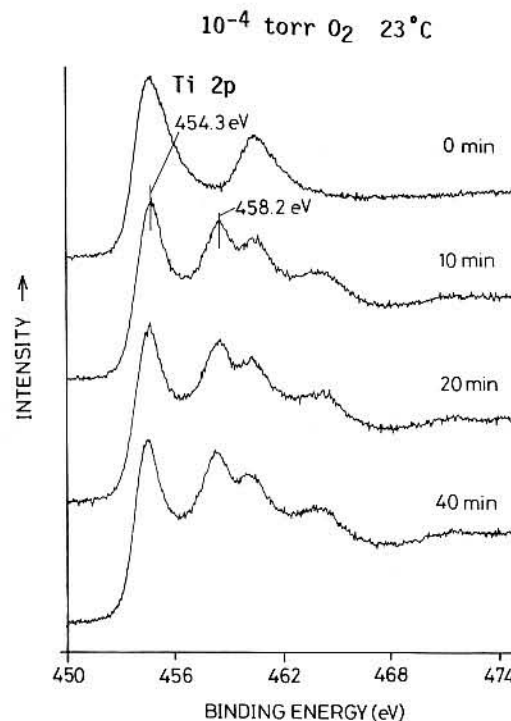


**Figure 2.** Ti 2p spectra of a sputtered-cleaned NiTi surface after different oxygen exposures at room temperature.

the end of the 40 min of oxygen exposure. The free energy of formation  $\Delta G$  (298 K) of NiO, TiO and  $TiO_2$  is  $-50.6$ ,  $-118.3$  and  $-212.6$  kcal mol<sup>-1</sup>, respectively, and these thermodynamic data strongly suggest that the oxidation of Ti is a much more favorable process than the oxidation of Ni. Preferential oxidation of one of the components in various alloys has been observed in many systems, including NiCo,<sup>1</sup> NiCr,<sup>4</sup> NiCrFe,<sup>4</sup> NiFe,<sup>15</sup> SnPb,<sup>16</sup> Pt<sub>3</sub>Ti<sup>10,17,18</sup> and Fe-18Cr-3Mo.<sup>19</sup>

**Table 1.** A summary of binding energies of titanium oxides from the literature

Material	Ti 2p <sub>3/2</sub> eV	Reference	Comments
Ti	453.8	13	Pure metal
	453.8	This work	NiTi
	455.2	15	Pt <sub>3</sub> Ti
	456.0	16	Pt <sub>3</sub> Ti
TiO	454.2	20	TiO <sub>x</sub> on Rh
	454.4	This work	NiTi
Ti <sub>2</sub> O <sub>3</sub>	455.6	10	Pt <sub>3</sub> Ti, TiO <sub>2</sub> present
	455.7	20	TiO <sub>x</sub> on Rh, TiO <sub>2</sub> present
	456.6	21	TiO <sub>2</sub> on Pt, TiO <sub>2</sub> present
	456.7	This work	NiTi, TiO <sub>2</sub> present
	456.8	17	Pt <sub>3</sub> Ti, TiO <sub>2</sub> present
TiO <sub>2</sub>	457.9	21	TiO <sub>2</sub> on Pt
	458.2	20	TiO <sub>x</sub> on Rh
	458.2	This work	NiTi
	458.6	21	TiO <sub>2</sub> on Pt, Ti <sup>3+</sup> present
	458.8	20	TiO <sub>x</sub> on Au
	458.8	This work	Ti <sup>3+</sup> present
	459.0	17	Pt <sub>3</sub> Ti, Ti <sup>3+</sup> present
459.1	20	TiO <sub>x</sub> on Rh, Ti <sup>3+</sup> present	
459.4	10	Pt <sub>3</sub> Ti, Ti <sup>3+</sup> present	

400 °C. The surface chemical composition of the alloy was studied by exposing a sputter-cleaned surface to  $10^{-4}$  Torr of oxygen at 400 °C for various lengths of time. Figures 3 and 4 show the Ni 2p and Ti 2p XPS spectra of the alloy, respectively, after different oxygen

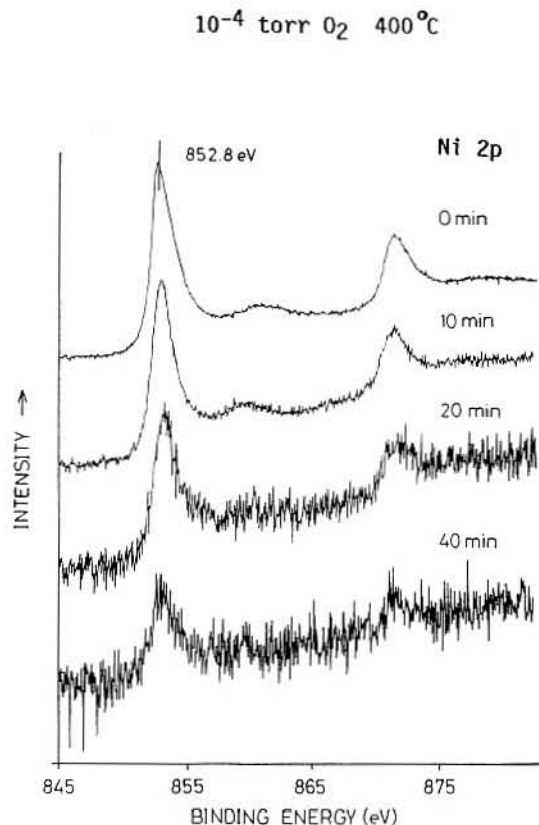


Figure 3. Ni 2p spectra of a sputtered-cleaned NiTi surface after different oxygen exposures at 400 °C and  $10^{-4}$  Torr of oxygen.

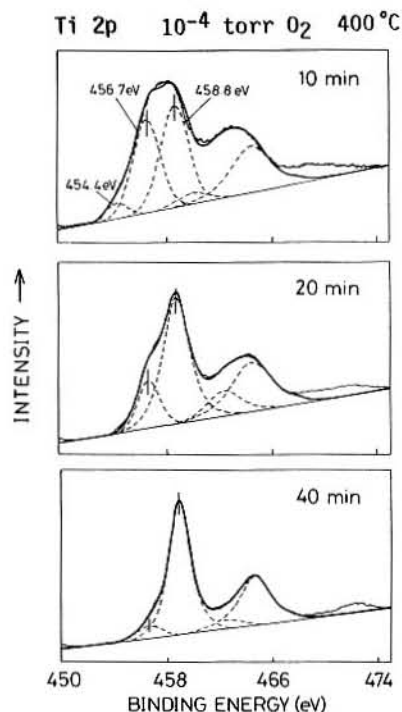


Figure 4. Ti 2p spectra of a sputtered-cleaned NiTi surface after different oxygen exposures at 400 °C and  $10^{-4}$  Torr of oxygen.

exposures. It was found that the Ti peak increased and the Ni peak decreased as a function of oxygen exposure. At the end of the 40 min of oxygen exposure, an almost complete layer of  $\text{TiO}_2$  was formed at the surface. It is interesting to note that Ni remained metallic even after 40 min of oxygen exposure, as shown in Fig. 3. On the contrary, in the Ti 2p spectra new peaks emerged, indicating the presence of different kinds of titanium oxides. Using the VG-5000 peak-synthesis program, three peaks were resolved and the peak positions were measured to be 454.4, 456.7 and 458.8 eV. The peaks at 454.4, 456.5 and 458.8 eV are identified as  $\text{TiO}$ ,  $\text{Ti}_2\text{O}_3$  and  $\text{TiO}_2$ , respectively, according to the available literature values of these oxides as summarized in Table 1. It has been reported by Paul *et al.*<sup>10</sup> that oxidation of  $\text{Pt}_3\text{Ti}$  at 737 °C and  $10^{-7}$  Torr of  $\text{O}_2$  produced surface with some  $\text{Ti}^{3+}$  ions, while oxidation at 377 °C produced only  $\text{TiO}_2$  in the form of islands. The presence of  $\text{Ti}^{3+}$  is explained by the formation of a higher portion of defects or uncoordinated ions in the surface region. These observations can be compared with those that we observed during the oxidation of NiTi at room temperature and 400 °C at low oxygen pressure. The formation of  $\text{Ti}_2\text{O}_3$  was only observed at 400 °C and not at room temperature. As shown in Table 1, we would like to point out that a significant shift in the binding energy of  $\text{Ti}^{4+}$  has been reported if  $\text{Ti}^{3+}$  is present. Our results also indicate that the presence of  $\text{Ti}^{3+}$  in the Ti oxide layer shifts the Ti 2p peak for  $\text{Ti}^{4+}$  to a higher binding energy, as reported previously.<sup>10,17,20,21</sup> However, during room-temperature oxidation,  $\text{Ti}^{3+}$  was not detected and the Ti 2p peak for  $\text{Ti}^{4+}$  was measured to be at a binding energy of 458.2 eV.

It can be concluded that oxygen-induced segregation of Ti is followed by preferential oxidation of the Ti at high temperatures. The diffusion rate of Ti at this temperature must be high enough to consume the available surface oxygen, thus preventing the oxidation of Ni even after 40 min of oxygen exposure. Preferential oxidation of one of the components, together with oxygen-induced segregation of the component with the larger oxygen affinity, has been reported for a few systems, including NiCr,<sup>4</sup> NiCrFe,<sup>4</sup> NiFe<sup>15</sup> and SnPb.<sup>16</sup>

### Atmospheric oxidation

**Room temperature.** Figures 5 and 6 show the Ni 2p and Ti 2p XPS spectra of the alloy, respectively, after various lengths of time in air. The oxygen concentration on the surface increased fairly slowly after a rapid rise during the first minute of air exposure. A key difference between low-pressure oxidation and atmospheric oxidation is the appearance of NiO after the first minute of air exposure (as shown in Fig. 5), while at low oxygen pressure, Ni remains metallic even after 40 min of exposure.

**450 °C.** Figures 7 and 8 show the survey and Ni 2p XPS spectra, respectively, when the sample was exposed to air at 450 °C for various lengths of time. After 1 min in air at 450 °C, there was a large increase in oxygen concentration and the Ni/Ti surface concentration ratio decreased approximately from 1.4 to 0.7. The binding energy of the Ni 2p peak shifted from 852.8 to 855.2 eV,

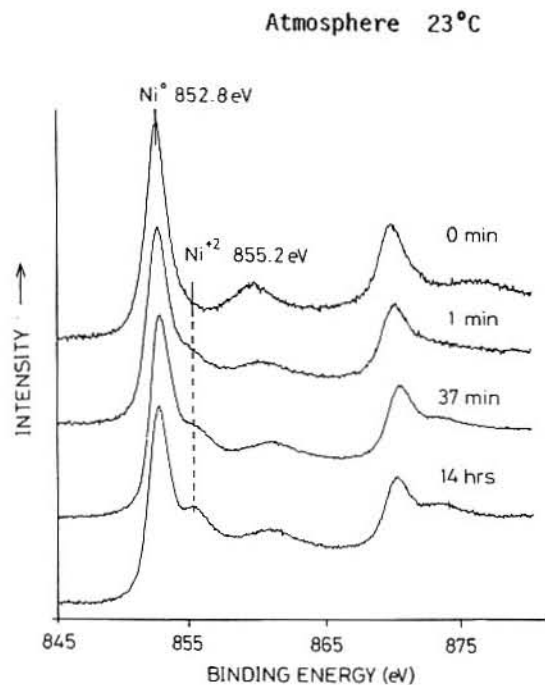


**Figure 5.** Ni 2p spectra of a sputtered-cleaned NiTi surface as a function of time at atmospheric pressure and room temperature.

indicating the formation of NiO. However, as shown in Fig. 8, we can still observe a low-energy shoulder in the Ni 2p peak, revealing the presence of metallic Ni after the first minute; while complete oxidation of Ti to TiO<sub>2</sub> was achieved within the same time. The binding energy of the Ti 2p peak for Ti<sup>4+</sup> was measured to be at 458.2 eV, suggesting the formation of a 'defect-free' TiO<sub>2</sub>. However, in this case, we did not observe the formation of a complete surface layer of TiO<sub>2</sub> even after 1 h.

Figures 9(a) and (b) show scanning electron micrographs of the surface before and after the first minute in air. After the first minute, patches of dark and light areas appeared on the surface. AES point analysis on

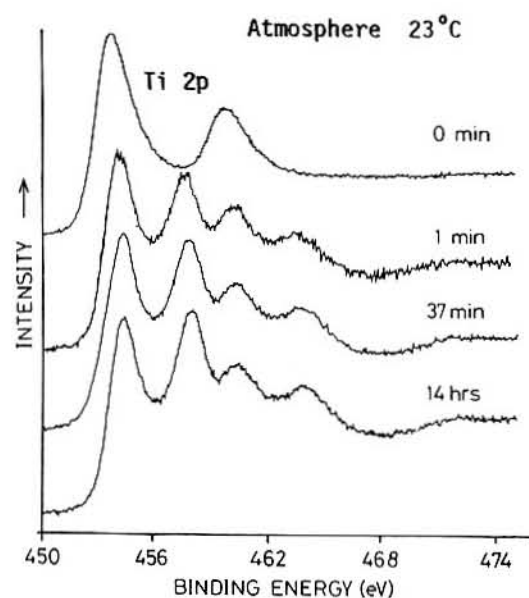


**Figure 6.** Ti 2p spectra of a sputtered-cleaned NiTi surface as a function of time at atmospheric pressure and room temperature.

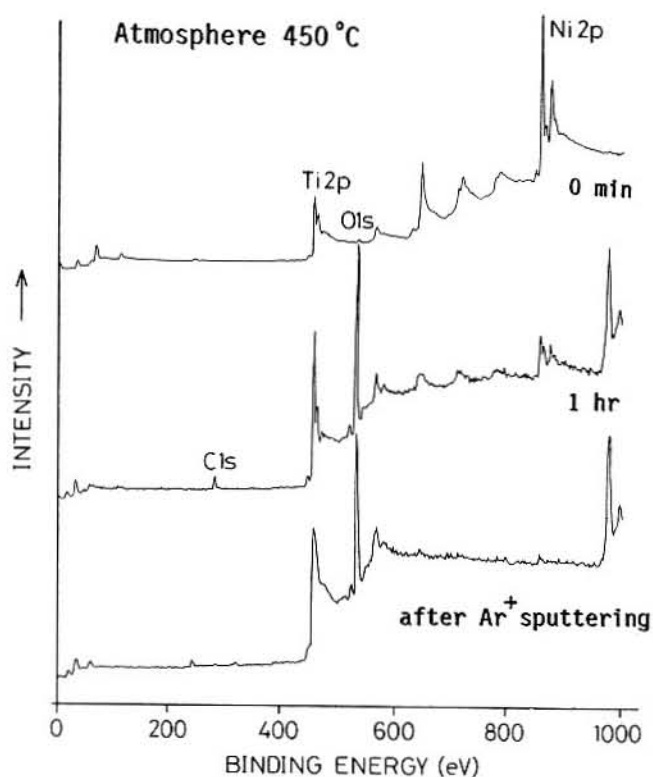


**Figure 7.** XPS spectra of a sputter-cleaned NiTi surface after different atmospheric exposures at 450°C and the resulting surface after 20 s of Ar<sup>+</sup> sputtering with the 3 cm ion gun.

the dark and light areas, as shown in Fig. 10, suggests that the dark areas are composed of TiO<sub>2</sub> only and the light areas are a mixture of NiO and TiO<sub>2</sub>. The presence of this mixture of NiO and TiO<sub>2</sub> on the top surface may explain for why we did not observe the for-

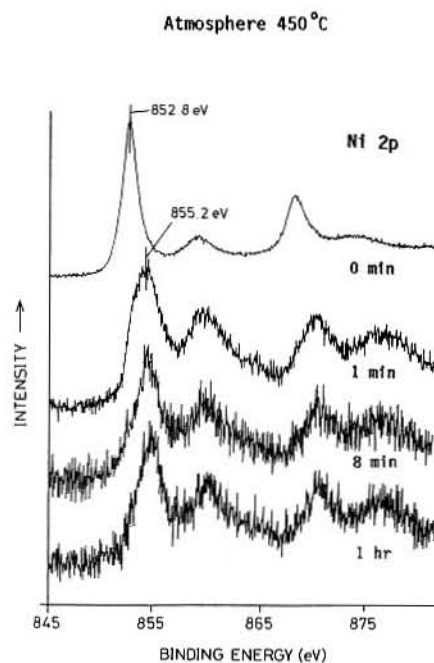


**Figure 8.** Ni 2p spectra for a sputtered-cleaned NiTi surface after different atmospheric exposures at 450°C.

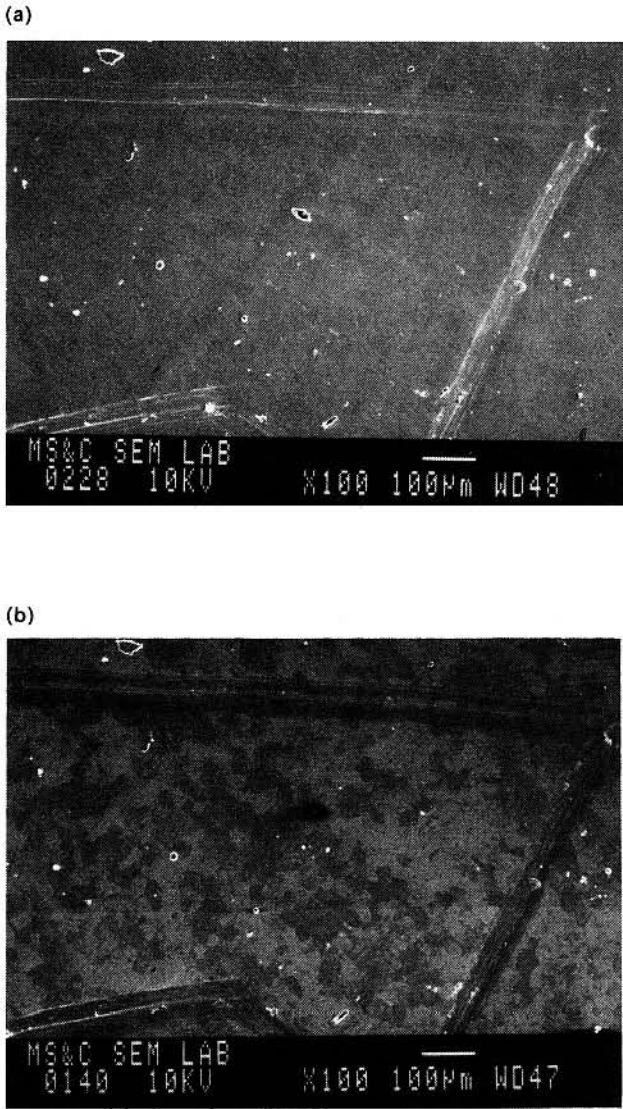


Figure 9. (a) SEM micrograph of a sputter-cleaned surface. The scratch was artificially introduced on the surface to mark a particular area for analysis. (b) SEM micrograph of the surface shown in (a) after 1 min in air at 450 °C.

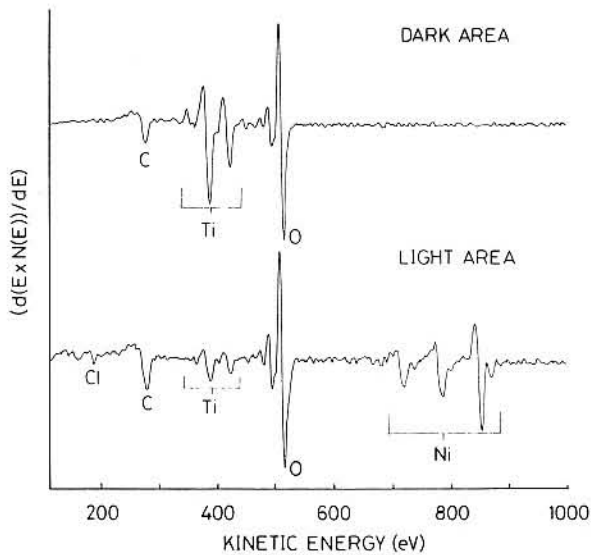


Figure 10. AES point analysis on a dark area and light area.

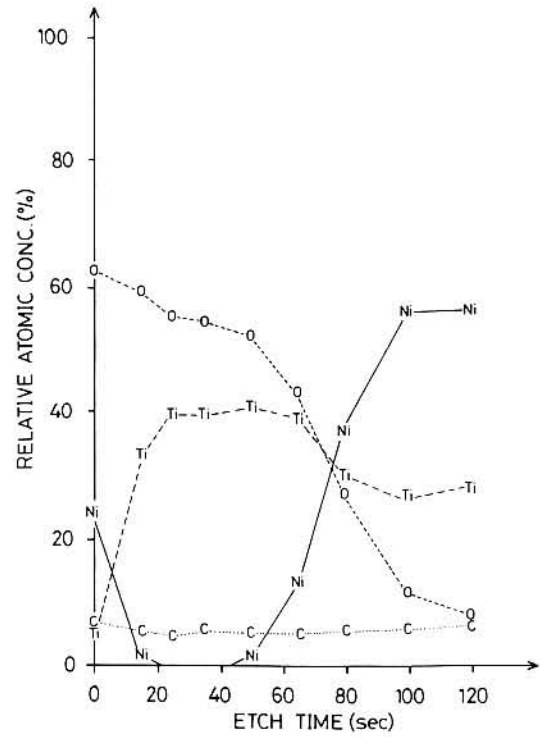


Figure 11. An XPS depth profile of a sample that has been oxidized in air at 450 °C for 1 h.

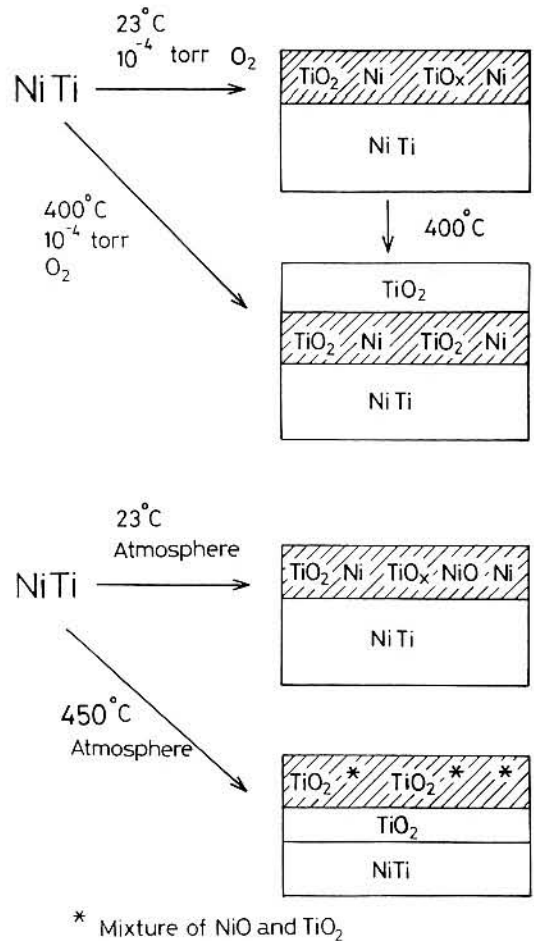


Figure 12. A schematic diagram showing oxidation processes at different oxygen exposures and temperatures.

mation of a complete layer of  $\text{TiO}_2$  on the surface, since these areas may act as barriers for Ti diffusion.

XPS depth profiling was performed on the sample that had been oxidized in air at  $450^\circ\text{C}$  for 1 h; the results are shown in Fig. 11. After 20 s of Ar sputtering (approximately equal to the removal of 48 Å of Au) with the 3 cm ion gun, only  $\text{TiO}_2$  was found on the surface, as shown in Fig. 8. This result suggests that a complete layer of  $\text{TiO}_2$  was formed underneath the top layer, which comprises areas containing  $\text{TiO}_2$  only and areas consisting of a mixture of  $\text{TiO}_2$  and NiO. After 100 s, the nickel concentration was approximately twice as high as that of titanium. These data tend to indicate that a nickel-rich layer is present underneath the  $\text{TiO}_2$  layer, although preferential sputtering of the titanium can contribute partially to the increase of the nickel concentration.

---

## CONCLUSIONS

---

- (1) At low oxygen pressure ( $10^{-4}$  Torr of oxygen) and room temperature, Ti is oxidized to form  $\text{TiO}_x$  and

$\text{TiO}_2$ , while Ni remains in the metallic form even after 40 min of oxygen exposure.

- (2) At  $400^\circ\text{C}$  and  $10^{-4}$  Torr of oxygen, oxygen-induced Ti segregation is accomplished with selective oxidation of Ti, resulting in a surface almost fully covered with  $\text{TiO}_2$ .
- (3) The results from low-pressure oxidation and atmospheric oxidation are very similar, except that the formation of NiO is observed after the first minute of air exposure.
- (4) At  $450^\circ\text{C}$  and atmospheric pressure, areas comprising a mixture of NiO and  $\text{TiO}_2$ , as well as areas comprising  $\text{TiO}_2$  only, are formed at the surface. Under this layer, a complete layer of  $\text{TiO}_2$  is found. Below the  $\text{TiO}_2$  layer, a nickel-rich layer is present.

Figure 12 presents a summary of the oxidation processes at different temperatures and oxygen pressures.

---

## REFERENCES

---

1. D. Majumdar, R. G. Spahn and J. S. Gau, *J. Electrochem. Soc.* **134**, 1825 (1987).
2. E. E. Hajcsar, Z. Z. He, P. R. Underhill and W. W. Smeltzer, *J. Vac. Sci. Technol.* **A6**, 3006 (1988).
3. E. E. Hajcsar, P. T. Dawson and W. W. Smeltzer, *Surf. Interface Anal.* **10**, 343 (1987).
4. J. Steffen and S. Hofmann, *Surf. Interface Anal.* **11**, 617 (1988).
5. S.-P. Jeng, P. H. Holloway, C. D. Batich and S. Hofmann, *J. Vac. Sci. Technol.* **A5**, 650 (1987).
6. E. W. A. Young, J. C. Riviere and L. S. Welch, *Surf. Sci.* **28**, 71 (1987).
7. E. W. A. Young, J. C. Riviere and L. S. Welch, *Appl. Surf. Sci.* **31**, 370 (1988).
8. A. M. Venezia and C. M. Loxton, *Surf. Interface Anal.* **11**, 287 (1988-89).
9. R. Van Noort, *J. Mater. Sci.* **22**, 3801 (1987).
10. J. Paul, S. D. Cameron, D. J. Dwyer and F. M. Hoffmann, *Surf. Sci.* **177**, 121 (1986).
11. M. Ask, J. Lausmaa and B. Kasemo, *Appl. Surf. Sci.* **35**, 283.
12. *Practical Surface Analysis by Auger and X-ray Photoelectron Spectroscopy*, ed. by D. Briggs and M. P. Seah. Wiley, Chichester (1983).
13. *Handbook of X-ray Photoelectron Spectroscopy*. Perkin-Elmer, Eden Prairie, MN (1979).
14. T. K. Hatwar and D. Chopra, *Surf. Interface Anal.* **7**, 93 (1985).
15. S. E. Greco, J. P. Roux and J. M. Blakely, *Surf. Sci.* **120**, 203 (1982).
16. G. C. Nelson and J. A. Borders, *J. Vac. Sci. Technol.* **20**, 939 (1982).
17. A. Dauscher, L. Hilaire, J. C. Spirlet, W. Müller and G. Maire, *Surf. Sci.* **204**, 161 (1988).
18. U. Bardi and P. N. Ross, *J. Vac. Sci. Technol.* **A2**, 1461 (1984).
19. M. Polak and B. Schiffmann, *J. Vac. Sci. Technol.* **A5**, 590 (1987).
20. M. E. Levin, M. Salmeron, A. T. Bell and G. A. Somorjai, *Surf. Sci.* **195**, 429 (1988).
21. D. J. Dwyer, S. D. Cameron and J. Gland, *Surf. Sci.* **159**, 430 (1985).